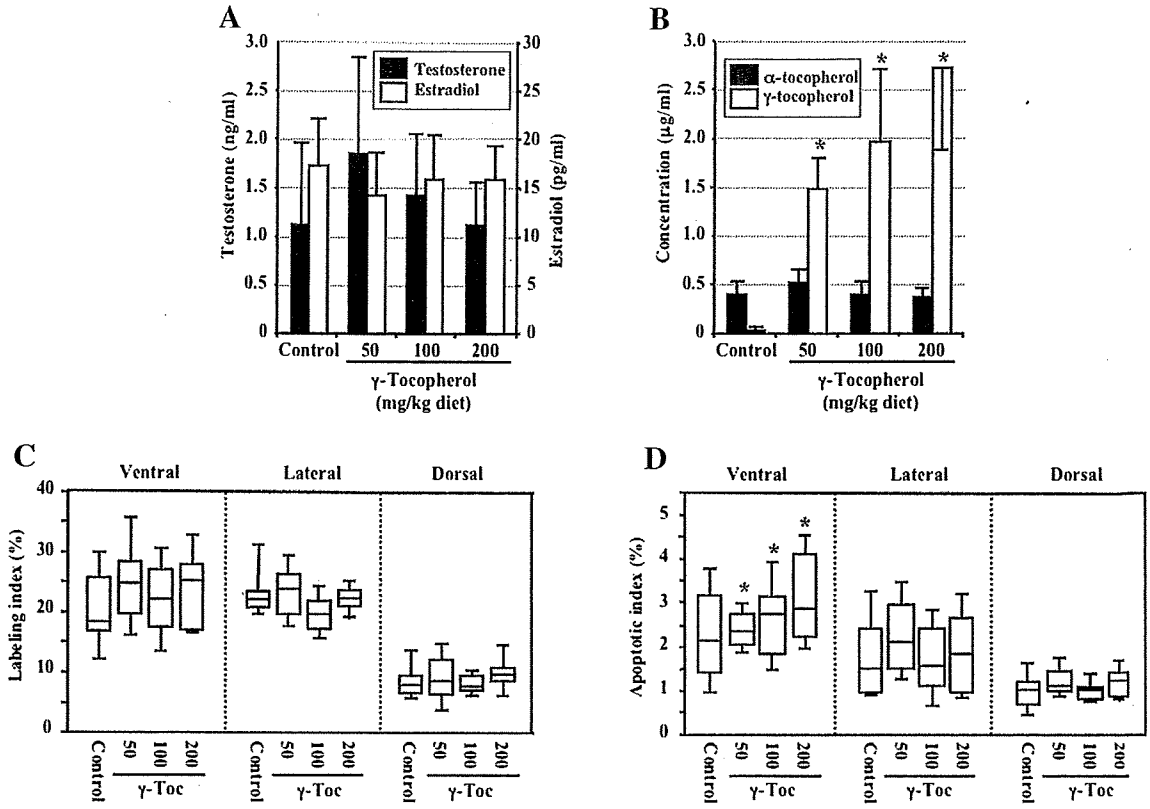

Fig. 3. Effects of γ-tocopherol on serum steroid hormones, plasma tocopherol levels, and labeling indices for Ki-67 and apoptotic cells (TUNEL) in individual prostatic lobes in Experiment 2. **A**: Serum levels of testosterone and estradiol. **B**: Plasma levels of tocopherols. Box plot data for (**C**) Ki-67 and (**D**) TUNEL indices in each prostate lobe of TRAP rats.

[31,32] but this controversial finding may be linked to particular biochemical activity and tissue distributions of the vitamin E isoform molecule. For instance, ingestion of α-tocopherol has been reported to result in reduction in the serum levels of γ-tocopherol [33–36]. In this context it should be noted that high serum concentrations of γ-tocopherols are associated with significantly lower risk of developing prostate cancer and protective effects of selenium and α-tocopherol were found only on the presence of high levels of γ-tocopherol [10].

In conclusion, the present investigation using the TRAP model provided clear evidence that γ-tocopherol can suppress prostate carcinogenesis with induction of apoptosis through caspase activation. In consideration of the lack of any toxic changes in organs such as the

TABLE IV. Quantitative Evaluation of Neoplastic Lesions in Prostates of TRAP Rats Treated With γ-Tocopherol (Experiment 2)

		Relative number of acini with histological characteristics (%)					
		Ventral lobe			Lateral lobe		
Treatment	No. of rats	LG-PIN	HG-PIN	ADC	LG-PIN	HG-PIN	ADC
Control	14	4.7 ± 1.6	92.3 ± 1.8	3.1 ± 0.8	19.1 ± 9.8	80.6 ± 9.7	0.4 ± 0.5
γ-Tocopherol 50 mg/kg	14	5.1 ± 2.4	93.1 ± 2.5	1.7 ± 1.4[a,c]	14.2 ± 6.0	85.5 ± 5.9	0.3 ± 0.3
γ-Tocopherol 100 mg/kg	14	4.8 ± 3.2	93.8 ± 2.9	1.4 ± 1.1[b,c]	12.5 ± 3.2	87.2 ± 3.1	0.2 ± 0.3
γ-Tocopherol 200 mg/kg	14	4.3 ± 1.9	94.2 ± 1.8	1.4 ± 0.8[b,c]	13.8 ± 5.9	86.0 ± 5.8	0.3 ± 0.3

LG-PIN, low grade prostatic intraepithelial neoplasia; HG, high grade; ADC, adenocarcinoma.
[a,b]$P < 0.05$ and 0.01 versus control, respectively.
[c]$P < 0.01$ versus control (Spearman's rank correlation coefficient test).

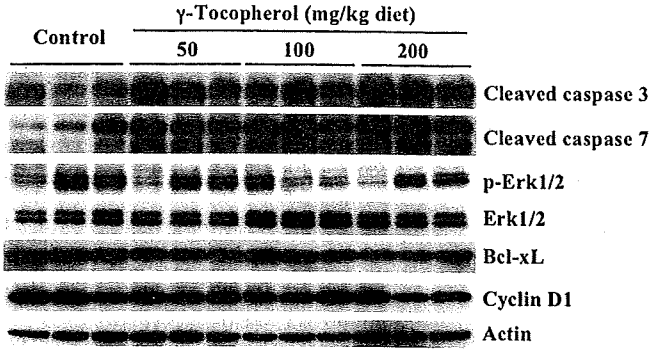

Fig. 4. Immunoblot analysis of caspases, MAPKs and other apoptosis-related proteins in ventral prostates of TRAP rats treated with γ-tocopherol in Experiment 2.

liver, kidneys, and heart, γ-tocopherol would appear to be a potential ideal agent for prostate cancer chemoprevention.

ACKNOWLEDGMENTS

This work was supported by a Grant-in-Aid for Cancer Research from the Ministry of Health, Labour and Welfare of Japan, a Grant-in-Aid for the 2nd Term Comprehensive 10-Year Strategy for Cancer Control from the Ministry of Health, Labour and Welfare of Japan and a grant from the Society for Promotion of Pathology of Nagoya, Japan.

REFERENCES

1. Parkin DM, Bray FI, Devesa SS. Cancer burden in the year 2000. The global picture. Eur J Cancer 2001;37:S4–S66.
2. Jemal A, Murray T, Ward E, Samuels A, Tiwari RC, Ghafoor A, Feuer EJ, Thun MJ. Cancer statistics, 2005. CA Cancer J Clin 2005; 55:10–30.
3. Franceschi S, La Vecchia C. Cancer epidemiology in the elderly. Crit Rev Oncol Hematol 2001;39:216–226.
4. Cunha GR, Donjacour AA, Cooks PS, Mee S, Bigsby RM, Higgins SJ, Sugimura Y. The endocrinology and developmental biology of the prostate. Endocr Rev 1987;8:338–362.
5. Denis LJ, Griffiths K. Endocrine treatment in prostate cancer. Semin Surg Oncol 2000;18:52–74.
6. Gronberg H. Prostate cancer epidemiology. Lancet 2003;361: 859–864.
7. Nelson WG, De Marzo AM, Isaacs WB. Prostate cancer. N Engl J Med 2003;349:366–381.
8. Shirai T, Asamoto M, Takahashi S, Imaida K. Diet and prostate cancer. Toxicology 2002;181–182:89–94.
9. Heinonen OP, Albanes D, Virtamo J, Taylor PR, Huttunen JK, Hartman AM, Haapakoski J, Malila N, Rautalahti M, Ripatti S, Maenpaa H, Teerenhovi L, Koss L, Virolainen M, Edwards BK. Prostate cancer and supplementation with α-tocopherol and β-carotene: Incidence and mortality in a controlled trial. J Natl Cancer Inst 1998;90:440–446.
10. Helzlsouer KJ, Huang H-Y, Alberg AJ, Hoffman S, Burke A, Norkus EP, Morris JS, Comstock GW. Association between α-tocopherol, γ-tocopherol, selenium, and subsequent prostate cancer. J Natl Cancer Inst 2000;92(24):2018–2023.
11. Huang H-Y, Alberg AJ, Norkus EP, Hoffman SC, Comstock GW, Helzlsouer KJ. Prospective study of antioxidant micronutrients in the blood and the risk of developing prostate cancer. Am J Epidemiol 2003;157:335–344.
12. Nomura AM, Stemmermann GN, Lee J, Craft NE. Serum micronutrients and prostate cancer in Japanese Americans in Hawaii. Cancer Epidemiol Biomarkers Prev 1997;6:487–491.
13. Weinstein SJ, Wright ME, Pietinen P, King I, Tan C, Taylor PR, Virtamo J, Albanes D. Serum α-tocopherol and γ-tocopherol in relation to prostate cancer risk in a prospective study. J Natl Cancer Inst 2005;97:396–399.
14. Asamoto M, Hokaiwado N, Cho YM, Takahashi S, Ikeda Y, Imaida K, Shirai T. Prostate carcinomas developing in transgenic rats with SV40 T antigen expression under probasin promoter control are strictly androgen dependent. Cancer Res 2001;61: 4693–4700.
15. Cho YM, Takahashi S, Asamoto M, Suzuki S, Inaguma S, Hokaiwado N, Shirai T. Age-dependent histopathological findings in the prostate of probasin/SV40 T antigen transgenic rats: Lack of influence of carcinogen or testosterone treatment. Cancer Sci 2003;94:153–157.
16. Said MM, Hokaiwado N, Tang M, Ogawa K, Suzuki S, Ghanem HM, Esmat AY, Asamoto M, Refaie FM, Shirai T. Inhibition of prostate carcinogenesis in probasin/SV40 T antigen transgenic rats by leuprorelin, a luteinizing hormone-releasing hormone agonist. Cancer Sci 2006;97:459–467.
17. Cho YM, Takahashi S, Asamoto M, Suzuki S, Tang T, Shirai T. Suppressive effects of antiandrogens, finasteride and flutamide on development of prostatic lesions in a transgenic rat model. Prostate Cancer Prost Dis 2007;10:378–383.
18. Seeni A, Takahashi S, Takeshita K, Tang M, Sugiura S, Sato SY, Shirai T. Suppression of prostate cancer growth by resveratrol in the transgenic rat for adenocarcinoma of prostate (TRAP) model. Asian Pac J Cancer Prev 2008;9:7–14.
19. Tang MX, Ogawa K, Asamoto M, Hokaiwado N, Seeni A, Suzuki S, Takahashi S, Tanaka T, Ichikawa K, Shirai T. Protective effects of citrus nobiletin and auraptene in transgenic rats developing adenocarcinoma of the prostate (TRAP) and human prostate carcinoma cells. Cancer Sci 2007;98:471–477.
20. Soeda S, Iwata K, Hosoda Y, Shimeno H. Daunorubicin attenuates tumor necrosis factor-α-induced biosynthesis of plasminogen activator inhibitor-1 in human umblical vein endothelial cells. Biochem Biophys Acta 2001;1538:234–241.
21. Galli F, Stabile AM, Betti M, Conte C, Pistilli A, Rende M, Floridi A, Azzi A. The effect of α- and γ-tocopherol and their carboxyethyl hydroxychroman metabolites on prostate cancer cell proliferation. Arch Biochem Biophys 2004;423(1):97–102.
22. Gysin R, Azzi A, Visarius T. γ-Tocopherol inhibits human cancer cell cycle progression and cell proliferation by down-regulation of cyclins. FASEB J 2002;16(14):1952–1954.
23. Jiang Q, Wong J, Fyrst H, Saba JD, Ames BN. γ-Tocopherol or combinations of vitamin E forms induce cell death in human prostate cancer cells by interrupting sphingolipid synthesis. Proc Natl Acad Sci USA 2004;101(51):17825–17830.
24. Yoshikawa S, Morinobu T, Hamamura K, Hirahara F, Iwamoto T. The effect of γ-tocopherol administration on α-tocopherol levels and metabolism in humans. Eur J Clin Nutr 2005;59:900–905.
25. Stone WL, Papas AM. Tocopherols and the etiology of colon cancer. J Natl Cancer Inst 1997;89:1006–1014.

26. Christen S, Woodall AA, Shigenaga MK, Southwell-Keely PT, Duncan MW, Ames BN. γ-Tocopherol traps mutagenic electrophiles such as NOx and complements α-tocopherol: Physiological implications. Proc Natl Acad Sci USA 1997;94:3217–3222.
27. Cooney RV, Franke AA, Harwood PJ, Hatch-Pigott V, Custer LJ, Mordan LJ. γ-Tocopherol detoxification of nitrogen dioxide: Superiority to α-tocopherol. Proc Natl Acad Sci USA 1997;90:1771–1775.
28. Hensley K, Benaksas EJ, Bolli R, Comp P, Grammas P, Hamdheydari L, Mou S, Pye QN, Stoddard MF, Wallis G. New perspectives on vitamin E: γ-tocopherol and carboxyethylhydroxychroman metabolites in biology and medicine. Free Rad Biol Med 2004;36(1):1–15.
29. Jiang Q, Ames BN. γ-Tocopherol, but not α-tocopherol, decreases proinflammatory eicosanoids and inflammation damage in rats. FASEB J 2003;17(8):816–822.
30. Jiang Q, Elson-Schwab I, Courtemanche C, Ames BN. γ-Tocopherol and its major metabolite, in contrast to α-tocopherol, inhibit cyclooxygenase activity in macrophages and epithelial cells. Proc Natl Acad Sci USA 2000;97(21):11494–11499.
31. Investigators THaH-TT. Effects of long-term vitamin E supplementation on cardiovascular events and cancer. JAMA 2005;293:1338–1347.
32. Lee I-M, Cook NR, Gaziano JM, Gordon D, Ridker PM, Manson JE, Hennekens CH, Buring JE. Vitamin E in the primary prevention of cardiovascular disease and cancer. JAMA 2005;294:56–65.
33. Handelman GJ, Machlin LJ, Fitch K, Weiter JJ, Dratz EA. Oral α-tocopherol supplements decrease plasma γ-tocopherol levels in humans. J Nutr 1985;115:807–813.
34. Li D, Saldeen T, Romeo F, Mehta JL. Relative effects of α- and γ-tocopherol on low-density lipoprotein oxidation and superoxide dismutase and nitric oxide synthase activity and protein expression in rats. J Cardiovasc Pharmacol Ther 1999;4:219–226.
35. Mahabir S, Coit D, Liebes L, Brady MS, Lewis JJ, Roush G, Nestle M, Fry D, Berwick M. Randomized, placebo-controlled trial of dietary supplementation of α-tocopherol on mutagen sensitivity levels in melanoma patients: A pilot trial. Melanoma Res 2002;12:83–90.
36. White E, Kristal AR, Shikany JM, Wilson AC, Chen C, Mares-Perlman JA, Masaki KH, Caan BJ. Correlates of serum α- and γ-tocopherol in the Women's Health Initiative. Ann Epidemiol 2001;11:136–144.

Pathology International 2009; **59**: 790–796 doi:10.1111/j.1440-1827.2009.02445.x

Original Article

Induction of apoptosis in the LNCaP human prostate carcinoma cell line and prostate adenocarcinomas of SV40T antigen transgenic rats by the Bowman–Birk inhibitor

MingXi Tang,* Makoto Asamoto, Kumiko Ogawa, Aya Naiki-Ito, Shinya Sato, Satoru Takahashi and Tomoyuki Shirai

Department of Experimental Pathology and Tumor Biology, Nagoya City University Graduate School of Medical Sciences, Nagoya, Japan

The soybean-derived serine protease inhibitor, Bowman–Birk inhibitor (BBI), has been reported as a potent chemoprevention agent against several types of tumors. The present study was undertaken to evaluate the effects of BBI on androgen-sensitive/dependent prostate cancers using a human prostate cancer cell (LNCaP) and the transgenic rats developing adenocarcinoma of the prostate (TRAP) model. Treatment of LNCaP prostate cancer cells with 500 μg/mL BBI resulted in inhibition of viability measured on WST-1 assays, with induction of connexin 43 (Cx43) and cleaved caspase-3 protein expression. Feeding of 3% roughly prepared BBI (BBIC) to TRAP from the age 3 weeks to 13 weeks resulted in significant reduction of the relative epithelial areas within the acinus and multiplicity of the adenocarcinomas in the lateral prostate lobes. Cx43- and terminal deoxynucleotidyl transferase mediated dUTP-biotin end labeling of fragmented DNA (TUNEL)-positive apoptotic cancer cells were more frequently observed in the lateral prostates treated with BBIC than in the controls. These *in vivo* and *in vitro* results suggest that BBI possesses chemopreventive activity associated with induction of Cx43 expression and apoptosis.

Key words: apoptosis, Bowman–Birk inhibitor, cancer, connexin 43, prostate

The incidence and mortality rates for prostate cancer are lower in Japanese and Chinese men with high consumption of soybean products in comparison with the Western population.[1,2] When Asian men migrate to the USA, however,, they and their next generations show marked increase of prostate cancers, suggesting that the differences in rates between Asian and US men are not solely due to genetic differences.[3] Indeed, dietary habits and lifestyle have been identified as major risk factors in prostate cancer growth and progression,[4,5] suggesting that some prostate cancer cases might be preventable by changing environmental factors.[6]

Intake of soybean products is associated with decreased risk of prostate cancer.[7–9] Possible chemopreventive substances in soybeans include the Bowman–Birk inhibitor (BBI) and a concentrated preparation (BBIC), enriched with this 71-amino acid protein (7.9 kDa), was found to be effective at suppressing cancer development in animals.[10] BBI has a well-characterized ability to block the catalytic activities of several serine proteases, including trypsin, chymotrypsin, cathepsin G, elastase, and chymase,[11] along with antioxidant properties related to potent anti-inflammatory activity.[12,13] Previous investigations showed BBI to be effective for prevention of generation of activated oxygen species in prostate cells,[14] and for activation of error-prone DNA repair through a p53-dependent mechanism.[15] These activities presumably inhibit the induction of DNA damage and/or facilitate its repair and thereby suppress genetic events leading to tumor initiation. Protease inhibitors have been shown to suppress carcinogenesis by affecting the levels of certain types of proteolytic activity or the expression of certain proto-oncogenes.[12] Both BBI and BBIC have been reported to inhibit the growth of LNCaP human prostate cancer xenografts in nude mice,[16] and are also reported to inhibit the growth, invasion, and clonogenic survival of human prostate cancer cells.[17] Another study showed that BBIC can reduce

Correspondence: Makoto Asamoto, MD, PhD, Department of Experimental Pathology and Tumor Biology, Nagoya City University Graduate School of Medical Sciences, 1 Kawasumi, Mizuho-cho, Mizuho-ku, Nagoya 467-8601, Japan. Email: masamoto@med.nagoya-cu.ac.jp

*Present address: Department of Pathology, Luzhou Medical College, SiChuan, China.

Received 3 March 2009. Accepted for publication 22 June 2009.

both prostate volume and prostate-specific antigen levels in patients with benign prostate hyperplasia.[18] Recently, it was reported that dietary administration of BBI inhibited *N*-methyl-*N*-nitrosourea (MNU) plus cyproterone acetate–testosterone propionate-induced prostate carcinogenesis in the rat dorsolateral prostate.[19] The present study was undertaken to investigate whether BBI might prevent the growth of prostate tumors with induction of connexin 43 (Cx43) in LNCaP cells, and in transgenic rats developing adenocarcinoma of the prostate (TRAP), which feature androgen receptor-positive and androgen-dependent prostate cancers.

MATERIALS AND METHODS

Cell culture and viability assay

Human androgen-sensitive prostate cancer LNCaP cells were purchased from the American Type Culture Collection (ATCC, Manassas, VA, USA) and maintained in T25 flasks with RPMI 1640 (Gibco, Carlsbad, CA, USA) containing 10% (V/V) heat-inactivated fetal bovine serum (FBS) and 0.5% penicillin/streptomycin in a 5% CO_2 atmosphere at 37°C in a humidified incubator. After growth of cells in 96-well plates (0.5×10^4 cells/well) to approximately 70% confluence, BBI (Sigma-Aldrich, St Louis, MO, USA) diluted in RPMI 1640 was added at concentrations of 500, 250, 125, 62.5, 31.3, 15.6, 7.8, 3.9, 2.0, 1.0 and 0 μg/mL. The effect of BBI on cell viability was determined using a 2-(4-iodophenyl)-3-(4-nitrophenyl)-5-(2,4-disulfophenyl)-2H-tetrazolium salt monosodium salt (WST-1) assay (Roche Applied Science, Mannheim, Germany). After 24 h treatment of BBI at the listed concentrations in a total 100 μL of culture medium in quadruplicate, 10 μL WST-1 was added to each well with incubation for 120 min at 37°C. Then each well was measured for absorbance at the wavelength of 430 nm. Percentage cell viability was determined relative to vehicle-treated control cells, arbitrarily assigned 100% viability.

Preparation of cell lysates and western blotting

LNCaP cells were plated in T25 flasks at 1×10^5 cells/flask in RPMI medium 1640. Seventy percent confluent cells were treated with BBI at dose of 500 μg/mL for the indicated time periods (0, 1, 3, 6, 12 and 24 h). Cells were collected into 85°C heated sodium dodecylsulfate-sample tubes with Cell Scrapers (Nunc, Rochester, NY, USA) and then frozen at −80°C until use. Samples were treated in 100°C for 10 min and then put on ice within 1 min. An aliquot of 10 μL of lysates of each sample was electrophoretically transferred to a nitrocellulose membrane (Amersham Bioscences, Buckinghamshire, UK). Non-specific binding on the membrane was minimized with 5% skim milk at room temperature for 1 h. Incubation was with primary antibodies (1:1000 dilution) overnight at 4°C followed by washing with PBST (1 × PBS/0.1% Tween 20, v/v, Pharmacia Biotech, Buckinghamshire, UK). The following primary antibodies were used: Monoclonal mouse anti-Cx43 purchased from Zymed Laboratories (South San Francisco, CA, USA); Polyclonal anti-cleaved caspase-3 and Caspase-3 obtained from Cell Signaling Technology (Danvers, MA, USA); Polyclonal rabbit anti-cyclin D1, P27 and BAX (Santa Cruz Biotechnology, Santa Cruz, CA, USA). After washing with PBST, the membranes were incubated with secondary antibodies for 1 h. Detection was performed using ECL and western blotting detection reagents (Amersham Biosciences, Piscataway, NJ, USA), and signals were detected with the Lumi-Imager system (Roche Molecular Biochemicals, Mannheim Germany).

Animals and chemicals

To produce transgenic offspring, transgenic homologous male rats, generated at Nagoya City University Graduate School of Medical Sciences with a Sprague–Dawley (SD) genetic background,[20,21] were bred with wild-type female SD rats (Clea, Tokyo, Japan). After weaning at 3 weeks of age, male rats were separated from female rats, and a tail biopsy was performed. Tail DNA, isolated by standard procedures, was used for determination of transgene incorporation by polymerase chain reaction as described previously.[20,22] All experimental male rats were housed three to a plastic cage on wood-chip bedding in an air-conditioned specific pathogen-free animal room at 22 ± 2°C and 55 ± 5% humidity with a 12 h light–dark cycle and fed soybean-free powdered basal diet (Oriental MF, Oriental Yeast, Tokyo, Japan), with or without test chemical, and water ad libitum. All animal studies were conducted in accordance with established guidelines and protocols approved by the Institutional Animal Care and Use Committee of Nagoya City University School of Medical Sciences. For the rat study, powdered BBIC (activity of trypsin inhibitor (TI): 260 U/g) was a gift from Fuji Oil (Osaka, Japan), as a soybean concentrate enriched in BBI.

Animal treatment, blood and tissue collection

A total of 24 male hetero-TRAP were divided into two groups (12 rats per group), receiving 3% BBIC or the soy-free basal powder diet (Oriental MF, Oriental Yeast) both mixed with 2% corn oil. The treatment dose of 3% (approx. 2000 mg/kg per day, according to the mean dietary consumption of rats) test compound for the animal study was chosen based on

previous chemopreventive studies,[23] in which BBIC had no significant effects on bodyweight, clinical pathology or organ weights in p53(+/–) (p53 knockout) mice. Starting at 3 weeks of age all of the animals were carefully inspected daily. Diet and water consumption was monitored twice a week. Bodyweights were recorded biweekly. At 13 weeks of age, all rats were killed. Under deep ether anesthesia, blood was collected from the abdominal aorta to measure testosterone and estrogen hormone levels. The accessory sex glands and urinary bladder were carefully removed from each rat. Prostates were removed and, after weighing, half of each ventral prostate was immediately frozen in liquid nitrogen for storage at –80°C. The remaining urogenital complex of each rat was harvested as a whole, together with the seminal vesicles, and fixed in 10% phosphate-buffered formalin. Livers, kidneys, spleens, lungs, testes and tongues were also excised, weighed and fixed. After fixation for 48 h, the remaining half of ventral lobes, dorsolateral prostate lobes containing urethra, anterior prostate lobes, and seminal vesicle was carefully dissected into individual lobes, and each was weighed. Tissues were embedded in paraffin, and stained with HE.

Histopathology, serum testosterone and estrogen levels and immunohistochemistry

Prostatic lesions, prostatic intra-epithelial neoplasm (PIN) and adenocarcinomas, were histopathologically diagnosed as described previously.[20,24] Because all of the TRAP developed multiple proliferative epithelial lesions in the present study, we performed a semi-quantitative analysis as follows: first, additional slides stained with Azan, showing clear contrast between epithelium and secreted material and stromal cells, were made. Then, relative areas of epithelium within acini were measured with the help of an Image Processor for Analytical Pathology (IPAP; Sumika Technos, Osaka, Japan).[24] According to the predominant morphology, each acinus was classified as normal, PIN or adenocarcinoma to evaluate the proportions. Testosterone and estrogen levels in the serum were analyzed using radioimmunoassays by a commercial laboratory (SRL, Tokyo, Japan). Immunohistochemistry for androgen receptor expression was performed with a Discovery instrument using DAB Map kits (Ventana Medical Systems, Tucson, AZ, USA) with polyclonal rabbit anti-androgen receptor (PA1-110; Affinity BioReagents, Golden, CO, USA) antibodies. For SV40 large T antigen, a mouse anti-SV40 large T antigen monoclonal antibody (Clone: PAb 101, BD PharMingen, San Diego, CA, USA), was applied. Binding was visualized with a Vectastain Elite ABC kit (Vector Laboratories, Burlingame, CA, USA) followed by light hematoxylin counterstaining to facilitate microscopy.

Expression of Cx43 in LNCaP

To confirm the Cx43 induction on immunohistochemistry in BBI-treated cells, we used a cell block method. Briefly, LNCap cells were treated with the BBI, and then collected into 15 mL tubes with Cell Scrapers (Nunc) at the indicated time points. After centrifugation at 300 *g* for 5 min and removal of medium, the samples were fixed with 20% buffered formalin at room temperature for 24 h and processed to make tissue samples. Immunohistochemistry for Cx43 expression was performed using a Discovery instrument with DAB Map kits (Ventana Medical Systems) and a polyclonal rabbit anti-Cx43 antibody.

Statistical analysis

Differences between BBI or BBIC treatment and vehicle control mean ± SD were analyzed on Student's *t*-test. $P < 0.05$ was taken as significant in all the experiments.

RESULTS

BBI inhibits the viability of androgen-sensitive LNCaP cells associated with induction of Cx43 and apoptosis

To gain insight into the possible mechanisms underlying BBI-induced chemopreventive effects on development of adenocarcinomas, we first evaluated the effects of BBI on viability of androgen-sensitive prostate cancer LNCaP cells using WST-1 assays (Fig. 1a), and then on Cx43 and cleaved caspase 3 as signals for apoptosis. As shown in Fig. 1(a), treatment with BBI at varying concentrations for 24 h caused dose-related reduction in viability, in agreement with an earlier observation.[17] As shown in Fig. 1(b), treatment at the dose of 500 μg/mL induced expression of Cx43 with a peak at 9 h after beginning the exposure, and this was confirmed on immunohistochemistry of cells at 6 h, the Cx43 proteins being predominantly localized to the BBI-treated LNCaP membranes (Fig. 1c,d). Treatment of BBI also induced an increase in cleaved caspase-3 expression with a peak at 9 h (Fig. 1b).

General observations in the animal experiment

Dietary administration of BBIC significantly reduced growth rate of bodyweight at 10 and 13 weeks of age ($P < 0.05$; Table 1), while increasing the relative weight of testes ($P < 0.05$) without affecting the relative weight of the liver, kidney and spleen (Table 1). Absolute weight of whole prostate and dorsolateral prostate, including urogenital organs, in the

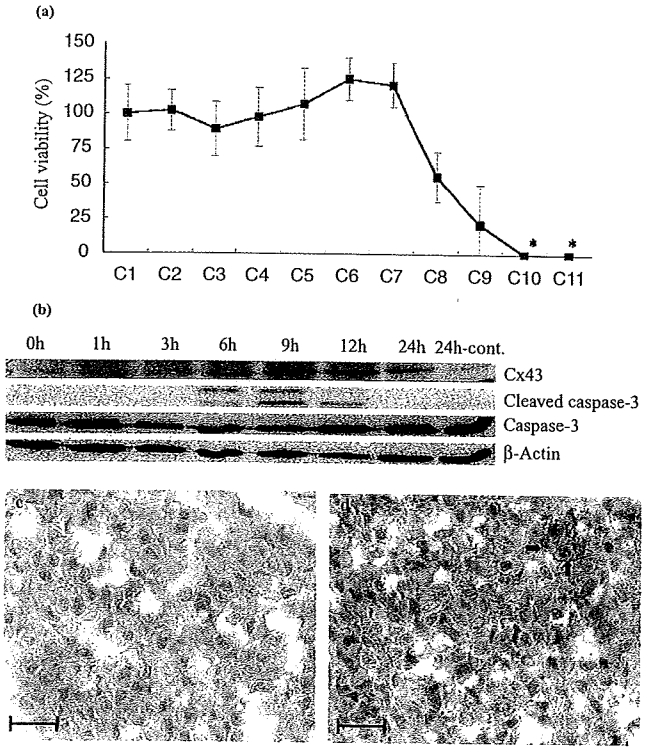

Figure 1 Effects of Bowman–Birk inhibitor (BBI) on cell viability, connexin 43 (Cx43) and cleaved caspase 3 expression in the LNCaP prostate cancer cell line. (**a**) Cells were exposed to a wide range of concentrations for 24 h and viability was determined by WST-1 assay. Results are given as a percentage of the vehicle-treated cell value treated as 100%. BBI caused significant dose-related growth inhibition. $^*P < 0.0001$ vs C1–C7. Concentrations of BBI: C1, 0 μg/mL; C2, 0.98 μg/mL; C3, 1.95 μg/mL; C4, 3.91 μg/mL; C5, 7.81 μg/mL; C6, 15.63 μg/mL; C7, 31.25 μg/mL; C8, 62.5 μg/mL; C9, 125 μg/mL; C10, 250 μg/mL; C11, 500 μg/mL. (**b**) Cells were treated with BBI (500 μg/mL) for the indicated period (0, 1, 3, 6, 12 and 24 h) and then whole-cell lysates were prepared and Cx43, caspase-3, cleaved caspase-3 expression levels were evaluated on western blot. (**c,d**) Immunohistochemistry for Cx43 expression. (**c**) No-treatment LNCaP at 6 h; (**d**) BBI-treated LNCaP at 6 h. Arrows, Cx43 proteins predominantly localized in the cell membranes. Bars, 20 μm.

BBIC treatment group was significantly lower than in the control group, but there were no changes in the relative weight of any of the individual prostate lobes (Table 2). Food and drinking water consumption were not affected (data not shown) and serum testosterone and estrogen levels remained unchanged (Table 1). Histologically, there were no pathological lesions suggesting toxicity of BBIC in the liver, kidneys, spleen, lung, pancreases or testes. All the animals developed prostate adenocarcinomas and PIN to various degrees so that there were no differences in incidence. On microscopy of HE staining tissues, however, the lateral prostate lobes of BBI-treated rats had lower numbers of adenocarcinoma and high-grade PIN acini, while low-grade PIN and normal glands were more frequently observed than in the control TRAP.

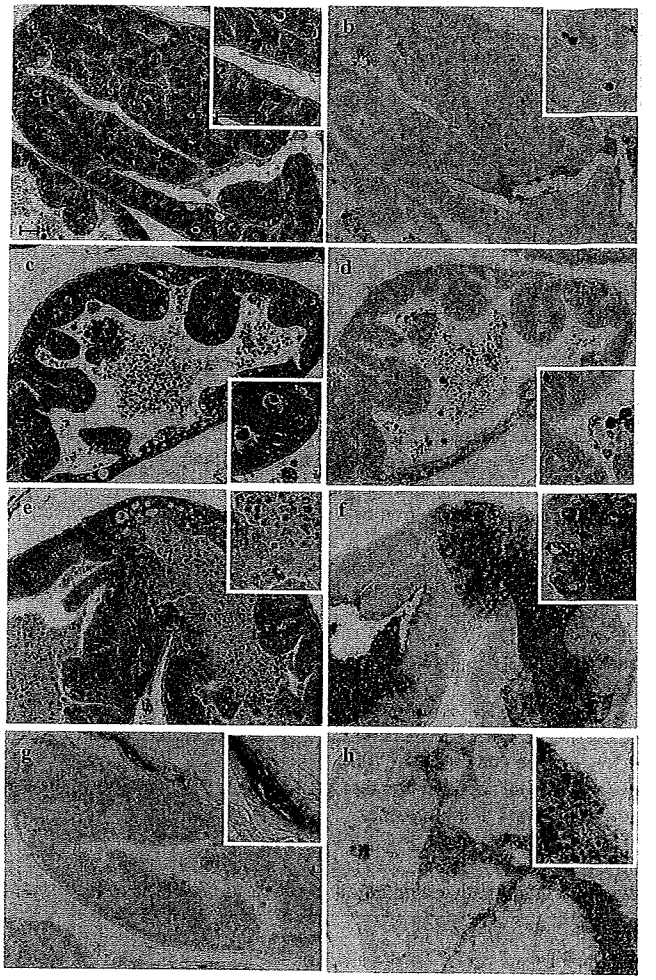

Figure 2 Representative histological appearance of the lateral prostates of transgenic rats developing adenocarcinoma of the prostate treated with vehicle control and concentrated preparation of Bowman–Birk inhibitor enriched with 3% soybean extract (BBIC). The BBI-treated lateral prostate is less dense, and the presence of luminal spaces or normal glands is more prominent. (**a**) The lateral prostate of the control rat is densely occupied by adenocarcinoma with reduced acinic lumina on HE staining. Inset: dividing cells. Bars, 20 μm. (**b**) Terminal deoxynucleotidyl transferase mediated dUTP-biotin end labeling of fragmented DNA (TUNEL) staining of the same area as in (a), indicating a few positive apoptotic calls. Inset: TUNEL-positive cells. Early stage BBIC effects with a few apoptotic cells evident on (**c**) HE and (**d**) TUNEL. Late-stage BBIC effects with many apoptotic cells on (**e**) HE and (**f**) TUNEL. (**c–f**) Inset: apoptotic cells. (**g**) Cx43 immunostaining: prostate cancer tissues in the control animals are negative with positive blood vessel cells. (**h**) Many Cx43-positive apoptotic cells are apparent in acini of prostate cancer tissues after treatment with BBIC. (**g,h**) Inset: larger image of (**g**) Cx43-positive blood vessel cells and (**h**) Cx43-positive apoptotic cells.

BBIC prevents the development of lateral prostate cancers

We determined the relative epithelial areas in each prostate acini to evaluate the extent of lesions. As shown in Table 3,

Table 1 Final body, organ weight and serum testosterone and estrogen concentration (mean ± SD)

No. rats	Bodyweight (g)	Relative organ weight (%) Liver	Kidney	Spleen	Testes	Testosterone (ng/mL)	Estrogen (pg/mL)
12	454 ± 9.8	4.1 ± 0.11	0.69 ± 0.02	0.19 ± 0.01	0.8 ± 0.02	2.33 ± 2.22	8.8 ± 3.11
11	421 ± 11.0*	4 ± 0.10	0.68 ± 0.01	0.20 ± 0.01	0.8 ± 0.02	2.70 ± 1.50	7.6 ± 2.33

*$P < 0.05$ vs control (Student's *t*-test).

Control, basal soybean-free diet + 2% corn oil; BBIC, 3% Bowman–Birk inhibitor in soybean-free diet + 2% corn oil.

Table 2 Final absolute and relative prostate weight (mean ± SD)

Treatment	No. rats	Whole prostate (g)	Ventral prostate (%) Absolute	Relative	Dorsolateral prostate (%) Absolute	Relative
Control	12	2.43 ± 0.07	0.26 ± 0.01	0.06 ± 0.00	0.700 ± 0.01	0.16 ± 0.00
BBIC	11	2.22 ± 0.06*	0.25 ± 0.02	0.06 ± 0.00	0.62 ± 0.01**	0.15 ± 0.01

*$P < 0.05$, **$P < 0.001$ vs control (Student's *t*-test).

Dorsolateral prostate includes the urogenital organs.

Control, basal soybean-free diet + 2% corn oil; BBIC, 3% Bowman–Birk inhibitor in soybean-free diet + 2% corn oil.

Table 3 Relative areas of the epithelial component within the acinus (mean ± SD)

Group	No. rats	Epithelium/Acinar (%) Ventral	Lateral	Dorsal	Anterior
Control	12	83.81 ± 2.79	72.72 ± 4.65	55.89 ± 5.16	25.67 ± 10.08
BBI	11	81.04 ± 6.43	65.28 ± 4.80*	54.26 ± 6.41	25.51 ± 10.71

*$P < 0.01$ vs control TRAP, Student's *t*-test.

Control, basal soybean-free diet + 2% corn oil; BBIC, 3% Bowman–Birk inhibitor in soybean-free diet + 2% corn oil; TRAP, transgenic rats developing adenocarcinoma of the prostate.

Table 4 Quantitative evaluation of prostate proliferative lesions (mean ± SD)

Treatment	No. rats	Acinus with predominant lesions (%) Normal	PIN	Adenocarcinoma
Ventral				
Control	12	0.02 ± 0.01	11.89 ± 5.01	88.11 ± 5.01
BBIC	11	0.02 ± 0.02	17.25 ± 16.16	82.75 ± 16.16
Lateral				
Control	12	6.51 ± 2.88	57.51 ± 14.70	35.98 ± 16.00
BBIC	11	12.18 ± 5.52**	71.35 ± 7.59*	16.47 ± 8.13**
Dorsal				
Control	12	50.93 ± 10.82	41.19 ± 10.25	7.88 ± 4.81
BBIC	11	44.35 ± 14.03	49.28 ± 14.45	6.37 ± 5.71

Significantly different from control TRAP: *$P < 0.05$, **$P < 0.01$.

Control, basal soybean-free diet + 2% corn oil; BBIC, 3% Bowman–Birk inhibitor in soybean-free diet + 2% corn oil; PIN, prostatic intra-epithelial neoplasm; TRAP, transgenic rats developing adenocarcinoma of the prostate.

dietary administration of BBIC significantly reduced the relative epithelial components of the lateral prostate lobes ($P < 0.05$) as compared with the control. Similar effects on the epithelial areas were also found in the ventral, dorsal and anterior prostate lobes, but were not statistically significant. Decrease in the proportion of adenocarcinoma acini ($P < 0.01$), and increase of PIN ($P < 0.05$) and normal ($P < 0.01$) acini were significant in BBIC-treated lateral prostate lobes compared with control TRAP (Table 4). Similar effects were also found in the ventral and dorsal prostate lobes, but without statistical significance (Table 4). In early stages of BBIC treatment, a few terminal deoxynucleotidyl transferase mediated dUTP-biotin end labeling of fragmented DNA (TUNEL)-positive cells were sometimes observed with white blood cell in acini (Fig. 2c,d). In the late stages, many apoptotic cells in acini were observed as TUNEL-positive apoptotic cells (Fig. 2e,f), to a greater extent than in the non-BBIC treatment group (Fig. 2a,b). In addition, on immunohistochemistry the Cx43-positive epithelial cells and exfoliated dead cells were more frequently observed in BBIC-treated rat prostates as compared with control rat prostates (Fig. 2g,h).

DISCUSSION

In the present *in vitro* experiments, treatment with BBI at a dose of 500 μg/mL caused increase in expression of Cx43 and cleaved caspase-3, but this became less prominent over time. It is known that BBI can be degraded by non-serine proteases produced by cells or even by some serine proteases that are not specifically inhibited by serine proteases actions.[17] Therefore, BBI may need to be replenished periodically to achieve the greatest possible inhibitory effect on LNCaP cells for induction of Cx43 and apoptosis. Cell–cell communication is important in homeostatic control of normal cell growth and differentiation, and alteration in gap-junction-mediated intercellular communication (GJIC) has been found to be related to carcinogenesis.[25] The present treatment with BBI induced induction of the major gap junction protein Cx43 expression, and the present results are similar to the inhibitory effects of BBI on the growth of osteosarcoma cells based on restoration of Cx43 expression.[26] Thus BBI may cause junctional communication among tumor cells, an alternative way to constrain neoplastic cell death. It has been reported that retroviral-mediated transfer of Cx43 into connexin-deficient LNCaP cells resulted in growth inhibition with cell differentiation, reduced tumorigenicity and gap junction formation.[27] In the present study, however, Cx43 expression was induced by the BBI. This indicates that Cx43 roles may change. Although BBI was found to possess some anti-apoptotic activity in mouse fibroblast C3H/10T1/2 cells,[28] in the present experiment with LNCaP cells the treatment of BBI was associated with induction of cleaved caspase-3 expression. Cx43 can increase the sensitivity of LNCaP to tumor necrosis factor-α-induced apoptosis,[29] and transfection of plasmid CMV-Cx43 into PC3 cells increased apoptosis and caspase-3 activity, in a GJIC-independent fashion.[30]

In the present *in vivo* study we demonstrated that BBIC significantly suppressed progression to adenocarcinomas in the lateral prostate lobes in TRAP, suggesting a potential for chemoprevention of human prostate cancer. There were no changes in serum androgen and estrogen levels, or in the labeling indices of androgen receptor and SV40 T antigen on immunohistochemistry of prostate tissues (data not shown), suggesting a mechanism of action through a non-androgen-mediated pathway, possibly related to the anti-proliferative activity of BBIC. There was no difference, however, in the BrdU labeling indices between the two groups (data not shown). In the *in vivo* prostate cancers, Cx43 expression was strong in dead prostate cancer cells after BBIC treatment (Fig. 2h).

Dietary administration of BBIC significantly reduced the bodyweight growth rate of TRAP without any clinical changes or histopathological lesions indicative of toxicity in any organs compared to the control rats. One of the mechanisms of anti-carcinogenesis of ingested protease inhibitors may involve an indirect effect through partial blocking of protein absorption,[31] which may relate to the decreased bodyweight of rats treated with BBIC in this experiment. There were no differences, however, in the relative weights of whole and dorsolateral prostates between the two TRAP groups and, in another study of BBI in rats, anti-carcinogenesis properties were evident without any bodyweight change.[19] It should be noted that high levels of trypsin inhibitors in the diet of rats can lead to bodyweight loss[32] but not in humans (or mice) because human trypsin is not strongly inhibited by soybean trypsin inhibitors.[33] Although we also found increase in the testes weights in the BBIC-treated TRAP rats, there were no related histopathological changes. These results may be compatible with previously reported findings using the osteosarcoma cell line U2OS showing negative growth control by BBI with induction of Cx43 expression.[26]

In conclusion, BBI treatment induced cell death with induction of Cx43 expression in the human prostate cancer LNCaP cells and *in vivo* in the TRAP prostate cancer model. *In vitro* and *in vivo*, BBI and BBIC effects regarding Cx43 and apoptosis are very similar. Similarly to the *in vitro* effects, BBI might affect prostate tissues *in vivo*, but the precise mechanisms need to be clarified before new curative and preventive materials for prostate cancers can be developed. The results strongly support the prostate cancer chemopreventive efficacy of a soybean diet including BBI, and further provide an insight into therapeutic implications of BBI for the treatment of prostate cancer with a focus on Cx43 expression.

ACKNOWLEDGMENTS

This research was supported partly by the Japan Health Sciences Foundation, a Grant-in-aid for Cancer Research from the Ministry of Health, Labour and Welfare of Japan, and a grant from the Society for Promotion of Pathology of Nagoya, Japan.

REFERENCES

1 Sipos E. Dietary trends for vegetable proteins in foods. *Inform* 1990; **1**: 753–7.
2 Giovannucci E. Epidemiologic characteristics of prostate cancer. *Cancer* 1995; **75**: 1766–77.
3 Cook LS, Goldoft M, Schwartz SM, Weiss NS. Incidence of adenocarcinoma of the prostate in Asian immigrants to the United States and their descendants. *J Urol* 1999; **161**: 152–5.
4 Kelloff GJ, Sigman CC, Greenwald P. Cancer chemoprevention: Progress and promise. *Eur J Cancer* 1999; **35**: 2031–8.
5 Bidoli E, Talamini R, Bosetti C *et al.* Macronutrients, fatty acids, cholesterol and prostate cancer risk. *Ann Oncol* 2005; **16**: 152–7.
6 Shirai T. Significance of chemoprevention for prostate cancer development: Experimental *in vivo* approaches to chemoprevention. *Pathol Int* 2008; **58**: 1–16.

7 Blumenfeld AJ, Fleshner N, Casselman B, Trachtenberg J. Nutritional aspects of prostate cancer: A review. *Can J Urol* 2000; **7**: 927–35; discussion 936.
8 Hebert JR, Hurley TG, Olendzki BC *et al.* Nutritional and socioeconomic factors in relation to prostate cancer mortality: A cross-national study. *J Natl Cancer Inst* 1998; **90**: 1637–47.
9 Fournier DB, Erdman JW Jr, Gordon GB. Soy, its components, and cancer prevention: A review of the *in vitro*, animal, and human data. *Cancer Epidemiol Biomarkers Prev* 1998; **7**: 1055–65.
10 Kennedy AR. The evidence for soybean products as cancer preventive agents. *J Nutr* 1995; **125**: 733S–743S.
11 Birk Y. The Bowman-Birk inhibitor. Trypsin- and chymotrypsin-inhibitor from soybeans. *Int J Pept Protein Res* 1985; **25**: 113–31.
12 Kennedy AR. The Bowman-Birk inhibitor from soybeans as an anticarcinogenic agent. *Am J Clin Nutr* 1998; **68**: 1406S–1412S.
13 Arbogast S, Smith J, Matuszczak Y *et al.* Bowman-Birk inhibitor concentrate prevents atrophy, weakness, and oxidative stress in soleus muscle of hindlimb-unloaded mice. *J Appl Physiol* 2007; **102**: 956–64.
14 Sun XY, Donald SP, Phang JM. Testosterone and prostate specific antigen stimulate generation of reactive oxygen species in prostate cancer cells. *Carcinogenesis* 2001; **22**: 1775–80.
15 Dittmann K, Virsik-Kopp P, Mayer C, Rave-Frank M, Rodemann HP. Bowman-Birk protease inhibitor activates DNA-dependent protein kinase and reduces formation of radiation-induced dicentric chromosomes. *Int J Radiat Biol* 2003; **79**: 801–8.
16 Wan XS, Ware JH, Zhang L *et al.* Treatment with soybean-derived Bowman Birk inhibitor increases serum prostate-specific antigen concentration while suppressing growth of human prostate cancer xenografts in nude mice. *Prostate* 1999; **41**: 243–52.
17 Kennedy AR, Wan XS. Effects of the Bowman-Birk inhibitor on growth, invasion, and clonogenic survival of human prostate epithelial cells and prostate cancer cells. *Prostate* 2002; **50**: 125–33.
18 Malkowicz SB, McKenna WG, Vaughn DJ *et al.* Effects of Bowman-Birk inhibitor concentrate (BBIC) in patients with benign prostatic hyperplasia. *Prostate* 2001; **48**: 16–28.
19 McCormick DL, Johnson WD. Chemoprevention of rat prostate carcinogenesis by soy isoflavones and by Bowman-Birk inhibitor. *Nutr Cancer* 2007; **57**: 148–93.
20 Asamoto M, Hokaiwado N, Cho YM *et al.* Prostate carcinomas developing in transgenic rats with SV40 T antigen expression under probasin promoter control are strictly androgen dependent. *Cancer Res* 2001; **61**: 4693–700.
21 Asamoto M, Hokaiwado N, Cho YM, Shirai T. Effects of genetic background on prostate and taste bud carcinogenesis due to SV40 T antigen expression under probasin gene promoter control. *Carcinogenesis* 2002; **23**: 463–7.
22 Said MM, Hokaiwado N, Tang M *et al.* Inhibition of prostate carcinogenesis in probasin/SV40 T antigen transgenic rats by leuprorelin, a luteinizing hormone-releasing hormone agonist. *Cancer Sci* 2006; **97**: 459–67.
23 Johnson WD, Dooley L, Morrissey RL *et al.* Oncogenicity evaluations of chemopreventive soy components in p53((+/–)) (p53 knockout) mice. *Int J Toxicol* 2006; **25**: 219–28.
24 Kandori H, Suzuki S, Asamoto M *et al.* Influence of atrazine administration and reduction of calorie intake on prostate carcinogenesis in probasin/SV40 T antigen transgenic rats. *Cancer Sci* 2005; **96**: 221–6.
25 Yamasaki H, Omori Y, Zaidan-Dagli ML *et al.* Genetic and epigenetic changes of intercellular communication genes during multistage carcinogenesis. *Cancer Detect Prev* 1999; **23**: 273–9.
26 Saito T, Sato H, Virgona N *et al.* Negative growth control of osteosarcoma cell by Bowman-Birk protease inhibitor from soybean; involvement of connexin 43. *Cancer Lett* 2007; **253**: 249–57.
27 Mehta PP, Perez-Stable C, Nadji M *et al.* Suppression of human prostate cancer cell growth by forced expression of connexin genes. *Dev Genet* 1999; **24**: 91–110.
28 Foehr MW, Tomei LD, Goddard JG, Pemberton PA, Bathurst IC. Antiapoptotic activity of the Bowman-Birk inhibitor can be attributed to copurified phospholipids. *Nutr Cancer* 1999; **34**: 199–205.
29 Wang M, Berthoud VM, Beyer EC. Connexin43 increases the sensitivity of prostate cancer cells to TNFalpha-induced apoptosis. *J Cell Sci* 2007; **120**: 320–29.
30 Fukushima M, Hattori Y, Yoshizawa T, Maitani Y. Combination of non-viral connexin 43 gene therapy and docetaxel inhibits the growth of human prostate cancer in mice. *Int J Oncol* 2007; **30**: 225–31.
31 Yavelow J, Finlay TH, Kennedy AR, Troll W. Bowman-Birk soybean protease inhibitor as an anticarcinogen. *Cancer Res* 1983; **43**: s2454–9.
32 Crass RA, Morgan RG. The effect of long-term feeding of soyabean flour diets on pancreatic growth in the rat. *Br J Nutr* 1982; **47**: 119–29.
33 Flavin DF. The effects of soybean trypsin inhibitors on the pancreas of animals and man: A review. *Vet Hum Toxicol* 1982; **24**: 25–8.

The Prostate 70:229–238 (2010)

Tranilast Suppresses Prostate Cancer Growth and Osteoclast Differentiation In Vivo and In Vitro

Shinya Sato,[1]* Satoru Takahashi,[1] Makoto Asamoto,[1] Taku Naiki,[1,2] Aya Naiki-Ito,[1] Kiyofumi Asai,[3] and Tomoyuki Shirai[1]

[1]Department of Experimental Pathology and Tumor Biology, Graduate School of Medical Sciences, Nagoya City University, Nagoya, Japan
[2]Department of Nephro-Urology, Graduate School of Medical Sciences, Nagoya City University, Nagoya, Japan
[3]Department of Molecular Neurology, Graduate School of Medical Sciences, Nagoya City University, Nagoya, Japan

BACKGROUND. In bone metastatic sites, prostate cancer cells proliferate on interacting with osteoclasts. Tranilast, which is used for an antiallergic drug, has been shown to inhibit growth of several cancers and stromal cells. The present study was conducted to assess suppressive effects of Tranilast on prostate cancer growth and osteoclast differentiation in vivo and in vitro.
METHODS. In vivo, rat prostate cancer tissue was transplanted onto cranial bones of F344 rats and Tranilast was given for 9 days at doses of 0, 200, or 400 mg/kg/day. In vitro, human prostate cancer cell lines, LNCaP, PC3, and DU145, the rat prostate cancer cell line, PLS-10, and rat bone marrow cells were similarly treated with the agent.
RESULTS. In vivo, tumor volumes were significantly decreased in the high dose group. While cell proliferation did not appear to be affected, apoptosis was induced and tumor necrosis was apparent. Cranial bone defects were decreased in the high dose group. In vitro, cell proliferation rates of all four cell lines were reduced by Tranilast and increased apoptosis was observed in LNCaP and PLS-10. In addition, Tranilast significantly reduced osteoclast differentiation of rat bone marrow cells. Western blot analysis of PLS-10 and LNCaP revealed that phospho-GSK3β was up-regulated and phospho-Akt was down-regulated.
CONCLUSIONS. Tranilast here suppressed rat prostate cancer growth and osteoclast differentiation. Growth of human prostate cancer cells was also inhibited. Thus, this agent deserves consideration as a candidate for conventional therapy of bone metastatic prostate cancer. *Prostate 70: 229–238, 2010.* © 2009 Wiley-Liss, Inc.

KEY WORDS: **Tranilast; bone microenvironment; prostate cancer; bone metastasis; osteoclast**

INTRODUCTION

Prostate cancer is the most common cancer among men in the United States [1], and is also becoming more frequent in Japan [2]. In advanced stages, patients frequently develop bone metastases and suffer from a variety of symptoms including bone pain, fractures, spinal cord compression, nerve root impingement, and bone marrow failure [3–5]. Therapeutic approaches such as radical prostatectomy and radiotherapy are curative for localized disease [6,7], but no curative treatments for bone metastatic prostate cancer are available. There is thus an urgent need for novel therapeutic approaches for the treatment of bone metastatic prostate cancer.

Generally, it is likely that cancer metastases depend on the interaction between tumor cells and stromal cells in the organ microenvironment [8,9]. In bone metastatic sites, prostate cancer cells interact with osteoclasts and osteoblasts, and proliferation is increased [10,11]. Consequently, inhibition of tumor cell growth as well

*Correspondence to: Shinya Sato, Department of Experimental Pathology and Tumor Biology, Graduate School of Medical Sciences, Nagoya City University, Nagoya 467-8601, Japan.
E-mail: satopin@med.nagoya-cu.ac.jp
Received 17 April 2009; Accepted 12 August 2009
DOI 10.1002/pros.21056
Published online 29 September 2009 in Wiley InterScience (www.interscience.wiley.com).

as osteoclast differentiation in the bone microenvironment can be considered important strategies for bone metastatic prostate cancer treatment.

Previously, we established transplantable rat prostate carcinomas from tumors that were originally induced by 3,2′-dimethyl-4-aminobiphenyl and testosterone propionate in F344 rats (PLS-P) [12,13]. Using PLS-P, we developed a syngenic rat model that shares characteristics with human prostate cancer bone metastasis regarding tumor–stromal interactions [14,15]. When PLS-P (androgen-independent, moderately differentiated adenocarcinoma) was transplanted onto the surface of rat calvaria, we observed osteolytic and osteoblastic changes at the tumor–bone interface, mimicking the histopathological features of bone metastases of human prostate cancer. Recently we used our animal model to provide evidence that osteoclasts contribute to growth of prostate cancer cells in the bone microenvironment by providing TGFβ from bone matrix [14,15], underlining its utility as a tool for examination of prostate carcinoma behavior in the bone microenvironment.

Tranilast, *N*-(3′4′-dimethoxycinnamonyl) anthranilic acid (*N*-5′), was developed in Japan as an antiallergic drug about 30 years ago [16]. Recently, it was found to inhibit proliferation of stromal cells such as fibroblasts, myofibroblasts and vascular smooth muscle cells in vitro and in vivo [17–21]. It also inhibits proliferation of desmoplastic tumors such as scirrhous gastric cancer and pancreatic cancer [22–24]. Furthermore tumor growth suppressive effects have been shown for various types of neoplasm [25–28].

Based upon the available findings, we hypothesized that Tranilast might suppress prostate cancer cell proliferation and osteoclast differentiation in the bone microenvironment. We therefore performed this in vitro/in vivo study using prostate cancer cell lines and rat bone marrow primary culture as well as our animal model.

MATERIALS AND METHODS

Animals

A total of 42 male rats of F344 were obtained at 5 weeks of age from Charles River Japan (Atsugi, Japan) for in vivo study, and three 4-week-old male rats were also obtained for rat bone marrow primary culture. All rats were maintained in plastic cages in an air-conditioned room at 22 ± 2°C and 55 ± 5% humidity. Food (Oriental MF; Oriental Yeast, Tokyo, Japan) and tap water were available ad libitum.

Tumor Tissue

PLS-P derived from carcinogen-induced rat prostate cancer was used in the present experiment as a transplantable prostate cancer. The details of the rat prostate cancer tissue are as previously reported [12–15].

Prostate Cancer Cell Lines

PC3, LNCaP, and DU145 were obtained from the American Type Culture Collection (ATCC). PLS-10, an androgen-independent rat prostate adenocarcinoma line established from PLS-P, was reported previously [29]. All four cell lines were maintained in RPMI 1640 media (Invitrogen, Carlsbad, CA) containing 10% FBS (Invitrogen) and 1% antibiotics (Antibiotic–Antimycotic, Invitrogen).

Animal Experiment

Approximately 0.3 g aliquots of PLS-P were transplanted onto cranial bones of 6-week-old male F344 rats under anesthesia. PLS-P was also transplanted subcutaneously into the flanks of F344 rats for evaluating the efficacy of Tranilast on prostate cancer in the subcutaneous microenvironment. For this, an incision of about 1 cm was made in the skin at the top of the head or the flank and a pocket beneath the skin was formed using forceps. The prostate tumor tissue was then inserted into the pocket, and the incision was closed using autoclips (BD Biosciences, Bedford, MA). Tumor sizes and body weights were measured every 3 days. One week after transplantation, autoclips were removed, and rats were divided into three groups (groups of rats with PLS-P transplanted onto the cranial bone; n = 8, groups of rats with PLS-P transplanted subcutaneously into the flank; n = 6). Tranilast (generously provided by KISSEI Pharmaceutical Co., Ltd, Nagano, Japan) was suspended in 0.5% methylcellulose solution (Wako, Osaka, Japan) and administered intragastrically at doses of 200 (low dose group) or 400 mg/kg/day (high dose group), once a day from day 9 to day 17 after tumor transplantation. In groups of rats with PLS-P transplanted subcutaneously into the flank, Tranilast was administered from day 9 to day 21 after transplantation. Rats in the control group received the methylcellulose vehicle alone. In groups of rats with PLS-P transplanted onto the cranial bone, at sacrificed on day 17, X-ray radiography of transplantation sites was performed with XED-125M (Shimazu, Tokyo, Japan), and cranial tumors with part of the calvarias were excised en bloc, fixed with 10% buffered formalin solution and processed for histological examination. For quantitative analysis of bone destruction, bone destruction length per total cranial bone length in hematoxylin and eosin (H&E) stained sections was examined under a light microscope connected to an image analysis system, the Image Processor for Analytical Pathology (IPAP, Sumika Technos Corp., Osaka, Japan), to provide a bone destruction index

(BDI). The research was conducted according to the Guidelines for the Care and Use of Laboratory Animals of Nagoya City University Medical School and the experimental protocol was approved by the Institutional Animal Care and Use Committee (H20-07).

Histochemistry and Immunohistochemistry

Specimens were sectioned (5 μm) and stained with H&E. To identify osteoclasts, tartrate-resistant acid phosphatase (TRAP) (Acid Phosphatase Leukocyte kit, Sigma-Aldrich, St. Louis, MO) was applied to paraffin sections. Multinuclear cells were stained by TRAP, and counted at the tumor–bone interface. To assess cell proliferation, sections were treated with Ki67 antibody (DAKO, Denmark) and sequentially with antirabbit secondary antibody and avidin–biotin complex (Vectastatin Elite ABC kit; Vector Laboratory, Burlingame, CA), then binding sites were visualized with diamino-benzidine. Sections were then counterstained with hematoxylin for microscopic examination. Proliferating cells were quantified counting Ki67-positive cells at a magnification of 400×. To identify apoptotic cells in the tumors, TdT-mediated dUTP-digoxigenin nick-end labeling (TUNEL) staining using a TUNEL assay kit (Takara, Shiga, Japan) was also performed on sections according to the manual. The apoptosis rate was calculated as the number of TUNEL positive tumor cells per total cell number at a magnification of 400× for three or four randomly selected areas. At least 1,000 cells were counted per lesion for the evaluation. TUNEL-positive cells and TUNEL-positive necrotic areas were assessed with the IPAP (Sumika Technos Corp.).

Rat Bone Marrow Primary Culture

Rat bone marrow cells were obtained from the tibiae of 4-week-old male rats as reported previously [15], seeded in 100-mm petri dishes (BD Biosciences, San Jose, CA) and cultured in α-MEM medium (Lonza, Switzerland) containing 10% FBS for 3 hr at 37°C. After incubation, the collected floating cells (osteoclast precursor cells) were cultured at 1.0×10^6 cells/ml/well in 24-well plates (Corning, Corning, NY) for 24 hr, then 10 ng/ml soluble RANKL (Wako), 0.1 ng/ml TGFβ (R&D Systems, Minneapolis, MN) and various concentrations of Tranilast (0, 0.001, 0.01, 0.1, and 1 mM) were added. The medium was refreshed after 3 days. After culturing for 1 week, cells were used for TRAP staining, and TRAP-positive multinucleated cells were counted.

Western Blot Analysis

PLS-10 and LNCaP treated with 1 mM Tranilast (most effective concentration for inhibiting cell proliferation and promoting apoptosis) for 1 hr were homogenized in RIPA buffer (150 mM NaCl, 50 mM Tris–HCl (pH 8.0), 1% NP-40, 0.5% sodium deoxycholate, 0.1% SDS, 1 mM phenylmethylsulphonyl fluoride, 1 mM sodium orthovanadate, and protease inhibitor cocktail (Roche, Mannheim, Germany)). Twenty micrograms aliquots of protein were resolved on SDS–PAGE and separated proteins were transferred to nitrocellulose membranes. The membranes were then incubated with the following antibodies: rabbit monoclonal antihuman and rat phospho-Akt (Thr308), phospho-Akt (Ser473), Akt, phospho-β-catenin (Ser33/37/Thr41), phosphor-β-catenin (Ser45), phospho-Bcl2, phospho-cMyc, phosphor-Erk5, phospho-FKHR, phospho-IκBα, phospho-JAK1, phosphor-NFκB, phospho-GSK3β (Ser9), GSK, phospho-p38MAPK, phospho-p42MAPK, phospho-PLCγ1, phospho-SAPK/JNK (these antibodies were purchased from Cell Signaling Technology, Lake Placid, NY), and β-actin (mouse monoclonal antibody, Sigma-Aldrich). Immunoreactions were demonstrated by the ECL-Plus detection system (GE Healthcare, Piscataway, NJ) after 1-hr incubation with secondary horseradish peroxidase-labeled antirabbit or antimouse antibodies (Cell Signaling Technology).

Cell Proliferation and Apoptosis Assays In Vitro

Cell proliferation of all 4 prostate cancer cell lines was assessed by WST-1 assay (Roche). Briefly, prostate cancer cells were plated in 96-well microplates at 1×10^4 cells/well in 100 μl of culture media and incubated for 24 hr with various concentrations of Tranilast (0, 0.001, 0.01, 0.1, and 1 mM) before exposure to 10 μl of WST-1 per the manufacturer's protocol. The formazan dye formed was quantified using a plate reader by the absorbance at 440 nm. Apoptosis of LNCaP and PLS-10 was assessed using a Guava Nexin kit and the Guava PCA system (Guava Technologies, Hayward, CA) utilizing two stains (annexin V and 7-amino actinomycin D [7-AAD]) to quantitate the percentage of apoptotic cells. The Nexin assay was performed according to the manufacturer's protocol with the following exception. Briefly, cells were incubated for 48 hr with various concentrations of Tranilast, and 1×10^6 cells/100 μl medium were then stained with annexin V and 7-AAD for 20 min on ice. Data were acquired on the Guava PCA system immediately.

RESULTS

Tumor Growth and Histological Analysis

Transplanted PLS-P grew to palpable size in 1 week after transplantation, adhering firmly to the calvaria in

all groups. Although the 0.3 g of transplanted tumor was palpable just after transplantation, the tumor was not palpable 2 or 3 days after transplantation. Then, after the transplanted tumor re-started growing, the tumor became palpable again about 1 week after transplantation. During the experimental period, mean body weights did not significantly differ among the groups, and no adverse signs such as diarrhea or weight loss were observed in Tranilast-treated groups. The tumor volume in the Tranilast high dose group was significantly decreased compared with that in the control group ($P = 0.018$, Fig. 1A). All palpable masses were histologically confirmed to be transplanted PLS-P tumors, and tumor cells invading the calvaria caused bone destruction (Fig. 1C). At the tumor–bone interface, extensive bone defects with many multinucleated cells and nodular osteoid formation with osteoblasts were observed (Fig. 1D). We also transplanted PLS-P subcutaneously into the flanks of F344 rats, and Tranilast was administered on the same schedule as the rats with cranial transplantation. The tumor volume in the Tranilast high dose group was also significantly decreased compared with that in the control group ($P = 0.033$, Fig. 1B).

Cell Proliferation and Apoptotic Rates for Prostate Tumors

Many Ki67-positive tumor cells were observed in tumors (Fig. 2A–C), but Ki67 positive cell indices did not reveal any differences in cell proliferation among the three groups (Fig. 2D). In the Tranilast high dose group, many TUNEL-positive cells were observed in the central region of the tumor (Fig. 3A). But in the control group, tumor cells had fewer TUNEL-positive cells (Fig. 3B). The percentage of TUNEL-positive cells and TUNEL-positive cell areas in tumors was significantly increased in the Tranilast high dose group ($P < 0.001$, Fig. 3C–F).

Degree of Bone Destruction by Prostate Tumor Invasion

Radiographs of cranial bone showed partial cranial bone defects at tumor transplanted sites (Fig. 4A). On histological analysis, the mean length of cranial bone defects in the Tranilast-high dose group was significantly decreased as compared to the control group ($P = 0.03$, Fig. 4B). Multinucleated cells in bone destruction sites were identified as osteoclasts by

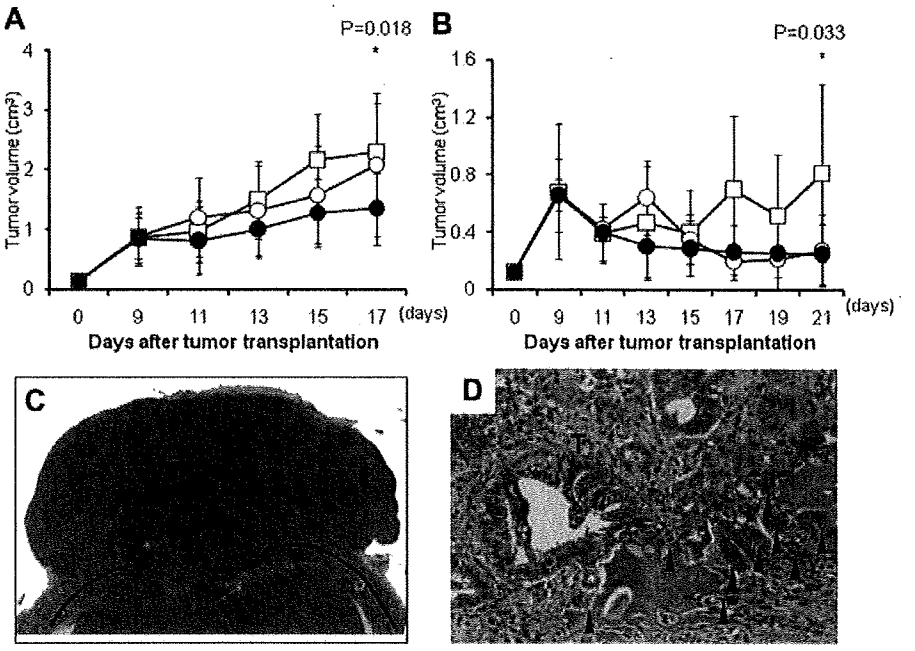

Fig. 1. Tumor growth and histological analysis of prostate cancer tissue on rat cranial bone. **A**,**B**: Sequential changes in cranial transplanted tumor volume (A) and subcutaneous transplanted tumor volume (B) (cm^3). Open squares, open circles, and closed circles represent the control group, Tranilast low dose group and Tranilast high dose group, respectively. Values are mean ± SD. **C**: Histological appearance of a tumor (T) invading and destroying rat cranial bone. The solid line indicates cranial bone and the dotted line indicates disrupted cranial bone. **D**: Higher magnification of the tumor–bone interface. Bone defects with multinucleated cells (arrowhead) are apparent with growth of a well-differentiated adenocarcinoma (T). C, 20× magnification. D, 200× magnification. [Color figure can be viewed in the online issue, which is available at www.interscience.wiley.com.]

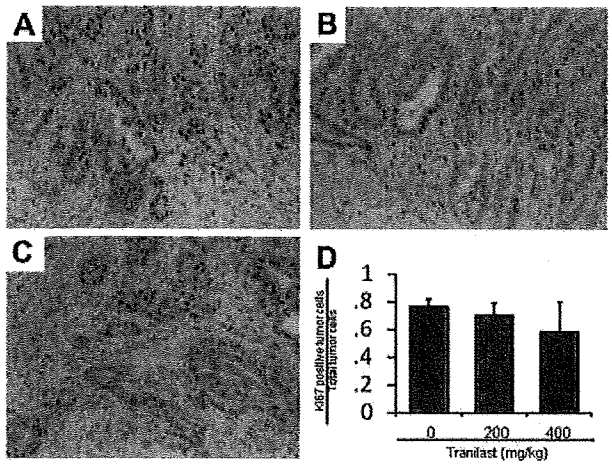

Fig. 2. Ki67 immunohistochemistry and labeling indices. **A–C**: Immunohistochemistry of Ki67 in the control group (A), Tranilast low dose group (B), and high dose group (C). Positive staining is evident in the nuclei of tumor cells. Ki67 positive cell labeling indices (mean ± SD values) are graphically presented in D. A–C: 200× magnification.

positive staining for TRAP (Fig. 4C). The numbers of multinucleated cells did not significantly differ among the three groups, but the multinucleated cell density per unit length (1 μm) of remaining cranial bone was marginally decreased in the Tranilast high dose group ($P = 0.078$, Fig. 4C).

Cell Proliferation and Apoptosis of Prostate Cancer Cells In Vitro

WST-1 assays revealed cell proliferation of all prostate cancer cell lines to be significantly decreased by Tranilast treatment at 0.1 and 1 mM ($P < 0.001$, Fig. 5A–D). The apoptotic cell ratios in the LNCaP and PLS-10 were increased in a Tranilast concentration-dependent manner (Fig. 5E).

Osteoclast Differentiation In Vitro

In the primary culture of rat bone marrow cells, the numbers of TRAP-positive multinucleated cells were significantly reduced by the high but not low dose of Tranilast (Fig. 6A–E).

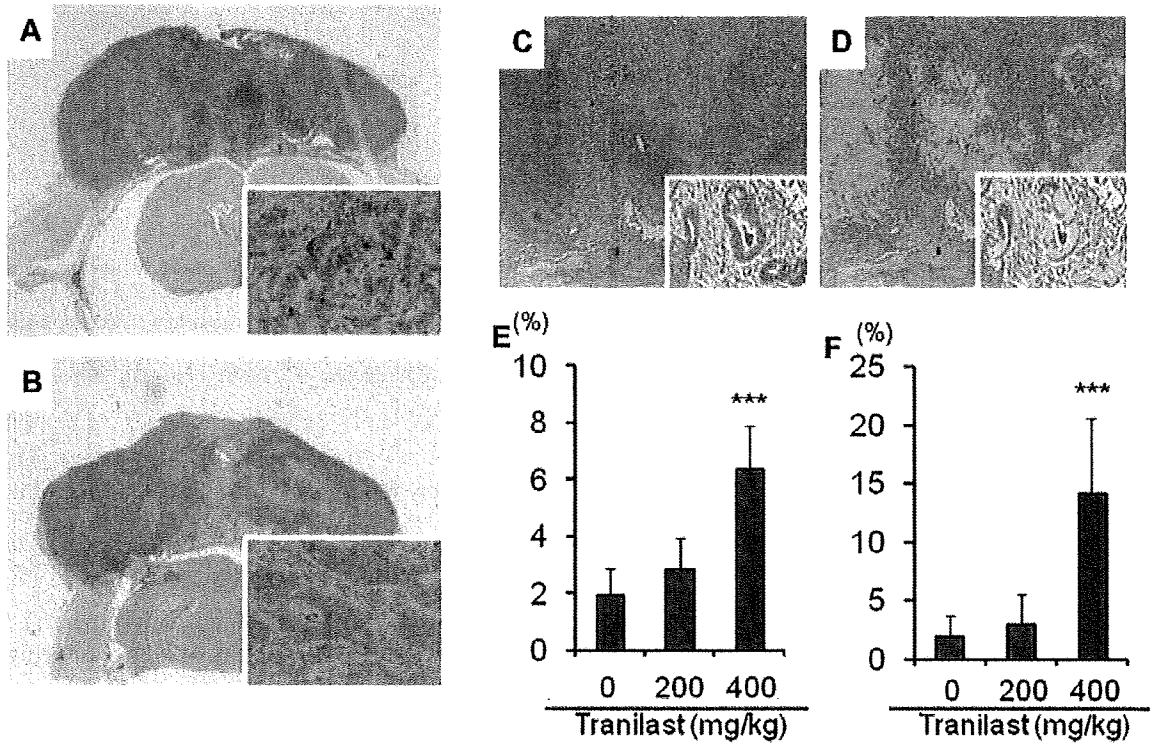

Fig. 3. TUNEL staining and labeling indices. **A,B**: TUNEL staining of tumor in Tranilast high-dose group (A) and the control group (B). Positive staining in the nuclei of tumor cells (inset). The TUNEL positive area (brown, **C**) was measured with an image analyzer (green, **D**). TUNEL positive cell labeling indices are presented in (**E**). **F**: The percentage TUNEL positive cell areas. Values are mean ± SD. ***$P < 0.001$ versus the control. A,B: 20× magnification. C,D: 100× magnification.

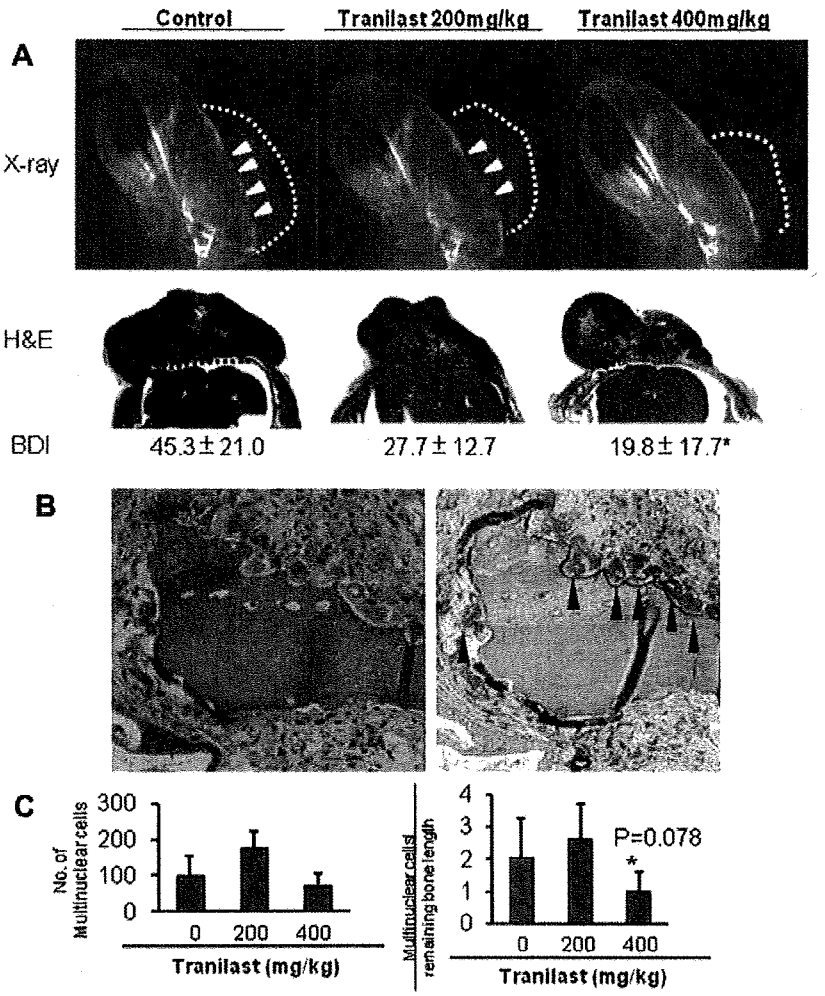

Fig. 4. Bone destruction and osteoclast induction in vivo. **A**: X-ray photographs and histological appearance of the tumor and rat cranial bone. In X-ray photographs, dotted lines indicate the tumor outline, and arrowheads indicate bone destruction. In the H&E stained section, the dotted line shows the area of bone destruction. BDI; destroyed bone length/total cranial bone length interacted with the tumor. **B**: Osteoclast induction in the tumor. Arrowheads indicate TRAP-positive multinucleated cells. **C**: The number of multinucleated cells (left graph) and the multinucleated cell density per unit length (1 μm) of cranial bone (right graph). *$P < 0.078$ versus the control. Values are mean ± SD. A, 10× magnification. B, 200× magnification.

Western Blot Analysis

Initially, we analyzed expression of several phosphorylated proteins associated with cell proliferation or apoptosis by Western blot (Fig. 7A). From the results, we chose pAkt as the most down-regulated and pGSK3β as the most up-regulated protein by Tranilast treatment, and Western blot analysis was carried out to determine the time course of GSK3β phosphorylation. As shown in Figure 7B, GSK3β phosphorylation at 1, 2, 6, and 12 hr after Tranilast treatment was increased in PLS-10 cells compared with the control value. Conversely, Thr (308) Akt phosphorylation at 1 hr after Tranilast treatment was decreased (Fig. 7C). Similar results were obtained with LNCaP cells (data not shown).

DISCUSSION

The present study demonstrated that Tranilast significantly suppresses rat prostate tumor growth on the cranial bone. Tranilast increased TUNEL positive cells in vivo and promote apoptosis in rat and human prostate cancer cells in vitro. Thus, it is clear that Tranilast has a potential to suppress prostate cancer growth by inducing apoptosis.

We chose doses of Tranilast in the in vivo study that were equivalent to the maximum doses in clinical use

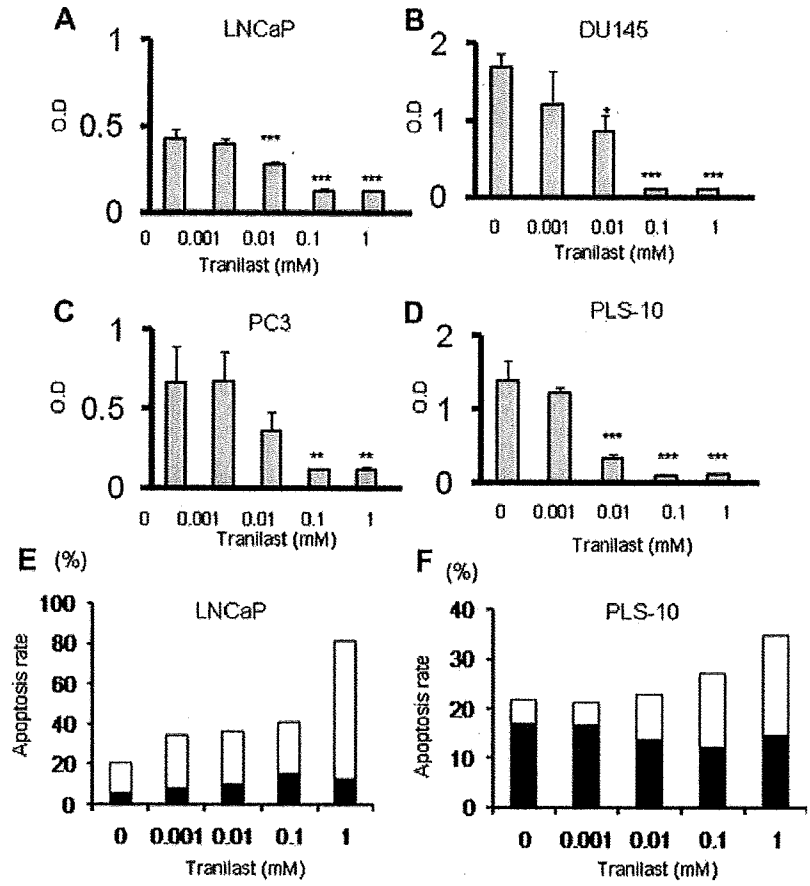

Fig. 5. Effects of Tranilast on cell proliferation and apoptosis of prostate cancer cell lines in vitro. WST-1 assay for analysis of cell proliferation in human (**A–C**, LNCaP, DU145, and PC3) and rat (**D**, PLS-10) prostate cancer cell lines. Data are mean ± SD values. **E,F**: The percentage of early cell apoptosis (white bar) and late cell apoptosis (black bar) of LNCaP (E) and PLS-10 (F). $^{**}P < 0.01$ versus the control. $^{***}P < 0.001$ versus the control.

[30] and chose concentrations of Tranilast in the in vitro study that were equivalent to the in vivo doses [31]. Although Tranilast dramatically suppressed the growth of cancer cells in vitro, it did not in the in vivo model. The reasons for this discrepancy are unknown but similar differences between in vivo and in vitro have also been found in other studies [32–37]. They mentioned this difference could be due to the three-dimensional nature of tumors in vivo as compared to the two-dimensional nature of monolayer cultures in vitro [32–34], and promotive effects of stromal cells on tumor cell proliferation in vivo [35–37]. In addition, we speculate that the inhibitory effect of Tranilast on prostate cancer cell proliferation in vivo was abrogated by the promoting effect of TGFβ on prostate cancer cell proliferation, which we have previously demonstrated [15].

As shown by Western blot analyses, Tranilast reduced Akt phosphorylation and induced GSK3β phosphorylation in rat and human prostate cancer cell lines. Akt phosphorylation is associated with promotion of proliferation of cancer cells including prostate cancer [38–40], and GSK3β phosphorylation is linked to inhibition of cell proliferation [41,42]. Thus, inhibitory effects of Tranilast on prostate cancer cell proliferation may be due to regulation of Akt and GSK3β phosphorylation.

Reduced bone destruction by Tranilast might further be considered at least partially due to growth inhibition of the tumors. Since osteoclast cell density per unit length of the bone was decreased by Tranilast, and osteoclast differentiation was clearly inhibited in vitro, the observed suppression of bone destruction might also be attributable to inhibition of osteoclast differentiation in the bone microenvironment.

Taken the results of the present study together, Tranilast may suppress prostate cancer growth and bone destruction by inducing tumor cell apoptosis and

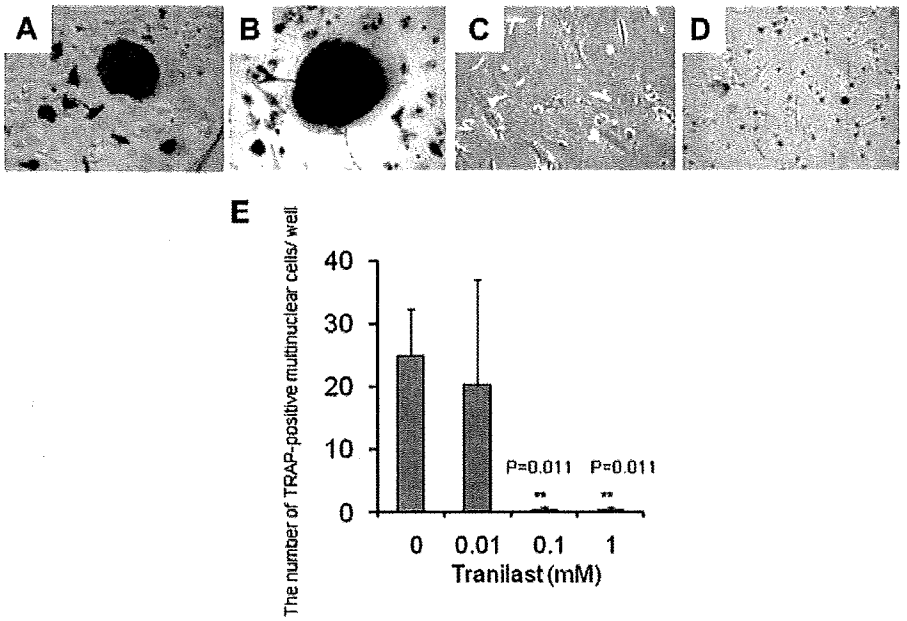

Fig. 6. Tranilast inhibits osteoclast differentiation. Rat bone marrow cells were cultured with control medium (**A**), Tranilast 0.01 mM (**B**), Tranilast 0.1 mM (**C**), and Tranilast 1 mM (**D**). The number of TRAP-positive multinucleated cells was significantly reduced by the high but not low dose (**E**). The averages of quadruplicate cultures for each group are graphically presented. Data are mean ± SD. A–E, 200× magnification. [Color figure can be viewed in the online issue, which is available at www.interscience.wiley.com.]

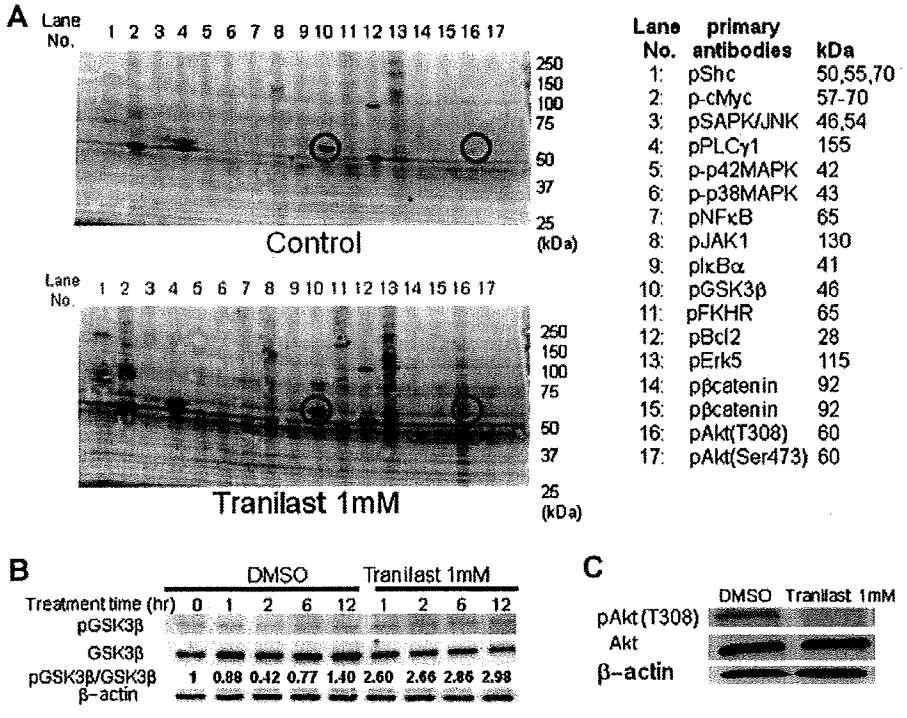

Fig. 7. Protein expression associated with cell proliferation and cell apoptosis in PLS-10. **A**: Western blot analysis of multiple proteins associated with cell proliferation and cell apoptosis. The lane numbers are for the primary antibodies on the right side. Significant spots were indicated with open squares. **B**: Chronological change of GSK3β phosphorylation on Western blotting. **C**: Expression of phosphorylated Akt on Western blotting. [Color figure can be viewed in the online issue, which is available at www.interscience.wiley.com.]

inhibiting osteoclast differentiation in the bone microenvironment.

CONCLUSIONS

Tranilast thus might provide additional therapeutic effects in combination with conventional drugs such as androgen antagonists, chemotherapeutic agents, and molecular target drugs. Further investigations are clearly warranted to explore Tranilast as a beneficial therapeutic option for prostate cancer patients with bone metastasis.

ACKNOWLEDGMENTS

We thank Junji Kuroda (KISSEI Pharmaceutical Co., Ltd, Nagano, Japan) for providing Tranilast. We would also like to thank Dr. Mitsuru Futakuchi, Department of Molecular Toxicology, Graduate School of Medical Sciences, for his excellent guidance and for his support in this project.

REFERENCES

1. Jemal A, Siegel R, Ward E, Hao Y, Xu J, Murray T, Thun MJ. Cancer statistics, 2008. CA Cancer J Clin 2008;58(2):71–96.
2. Qiu D, Katanoda K, Marugame T, Sobue T. A Joinpoint regression analysis of long-term trends in cancer mortality in Japan (1958–2004). Int J Cancer 2009;124(2):443–448.
3. Major PP, Cook RJ, Chen BL, Zheng M. Survival-adjusted multiple-event analysis for the evaluation of treatment effects of zoledronic Acid in patients with bone metastases from solid tumors. Support Cancer Ther 2005;2(4):234–240.
4. Coleman RE. Clinical features of metastatic bone disease and risk of skeletal morbidity. Clin Cancer Res 2006;12 (20 Pt 2):6243s–6249s.
5. Brescia FJ, Portenoy RK, Ryan M, Krasnoff L, Gray G. Pain, opioid use, and survival in hospitalized patients with advanced cancer. J Clin Oncol 1992;10(1):149–155.
6. Taplin ME, Xie W, Bubley GJ, Ernstoff MS, Walsh W, Morganstern DE, Regan MM. Docetaxel, estramustine, and 15-month androgen deprivation for men with prostate-specific antigen progression after definitive local therapy for prostate cancer. J Clin Oncol 2006;24(34):5408–5413.
7. Speight JL, Roach M III. Advances in the treatment of localized prostate cancer: The role of anatomic and functional imaging in men managed with radiotherapy. J Clin Oncol 2007;25(8):987–995.
8. Bogenrieder T, Herlyn M. Axis of evil: Molecular mechanisms of cancer metastasis. Oncogene 2003;22(42):6524–6536.
9. Tuma RS. Mechanisms of metastasis: Theories focus on microenvironment, host factors, genes. J Natl Cancer Inst 2008;100(24):1752–1754.
10. Mundy GR. Mechanisms of bone metastasis. Cancer 1997;80(Suppl 8):1546–1556.
11. Roodman GD. Mechanisms of bone metastasis. N Engl J Med 2004;350(16):1655–1664.
12. Shirai T, Tamano S, Kato T, Iwasaki S, Takahashi S, Ito N. Induction of invasive carcinomas in the accessory sex organs other than the ventral prostate of rats given 3,2′-dimethyl-4-aminobiphenyl and testosterone propionate. Cancer Res 1991;51(4):1264–1269.
13. Kato KTS, Mori S, Futakuchi M, Cui L, Ito N, Shirai T. Establishment of transplantable rat prostate carcinomas from primary lesions induced by 3, 2′-dimethyl-4-aminobiphenyl and testosterone. J Toxicol Pathol 1998;11:27–32.
14. Lynch CC, Hikosaka A, Acuff HB, Martin MD, Kawai N, Singh RK, Vargo-Gogola TC, Begtrup JL, Peterson TE, Fingleton B, Shirai T, Matrisian LM, Futakuchi M. MMP-7 promotes prostate cancer-induced osteolysis via the solubilization of RANKL. Cancer Cell 2005;7(5):485–496.
15. Sato S, Futakuchi M, Ogawa K, Asamoto M, Nakao K, Asai K, Shirai T. Transforming growth factor beta derived from bone matrix promotes cell proliferation of prostate cancer and osteoclast activation-associated osteolysis in the bone microenvironment. Cancer Sci 2008;99(2):316–323.
16. Azuma H, Banno K, Yoshimura T. Pharmacological properties of N-(3′,4′-dimethoxycinnamoyl) anthranilic acid (N-5′), a new anti-atopic agent. Br J Pharmacol 1976;58(4):483–488.
17. Isaji M, Nakajoh M, Naito J. Selective inhibition of collagen accumulation by N-(3,4-dimethoxycinnamoyl)anthranilic acid (N-5′) in granulation tissue. Biochem Pharmacol 1987;36(4):469–474.
18. Miyazawa K, Kikuchi S, Fukuyama J, Hamano S, Ujiie A. Inhibition of PDGF- and TGF-beta 1-induced collagen synthesis, migration and proliferation by tranilast in vascular smooth muscle cells from spontaneously hypertensive rats. Atherosclerosis 1995;118(2):213–221.
19. Isaji M, Miyata H, Ajisawa Y, Takehana Y, Yoshimura N. Tranilast inhibits the proliferation, chemotaxis and tube formation of human microvascular endothelial cells in vitro and angiogenesis in vivo. Br J Pharmacol 1997;122(6):1061–1066.
20. Isaji M, Aruga N, Naito J, Miyata H. Inhibition by tranilast of collagen accumulation in hypersensitive granulomatous inflammation in vivo and of morphological changes and functions of fibroblasts in vitro. Life Sci 1994;55(15):PL287–PL292.
21. Suzawa H, Kikuchi S, Arai N, Koda A. The mechanism involved in the inhibitory action of tranilast on collagen biosynthesis of keloid fibroblasts. Jpn J Pharmacol 1992;60(2):91–96.
22. Yashiro M, Chung YS, Sowa M. Tranilast (N-(3,4-dimethoxycinnamoyl) anthranilic acid) down-regulates the growth of scirrhous gastric cancer. Anticancer Res 1997;17(2A):895–900.
23. Murahashi K, Yashiro M, Inoue T, Nishimura S, Matsuoka T, Sawada T, Sowa M, Hirakawa-Ys Chung K. Tranilast and cisplatin as an experimental combination therapy for scirrhous gastric cancer. Int J Oncol 1998;13(6):1235–1240.
24. Hiroi M, Onda M, Uchida E, Aimoto T. Anti-tumor effect of N-[3,4-dimethoxycinnamoyl]-anthranilic acid (tranilast) on experimental pancreatic cancer. J Nippon Med Sch 2002;69(3):224–234.
25. Nie L, Oishi Y, Doi I, Shibata H, Kojima I. Inhibition of proliferation of MCF-7 breast cancer cells by a blocker of Ca(2+)-permeable channel. Cell Calcium 1997;22(2):75–82.
26. Yatsunami J, Aoki S, Fukuno Y, Kikuchi Y, Kawashima M, Hayashi SI. Antiangiogenic and antitumor effects of tranilast on mouse lung carcinoma cells. Int J Oncol 2000;17(6):1151–1156.
27. Platten M, Wild-Bode C, Wick W, Leitlein J, Dichgans J, Weller M. N-[3,4-dimethoxycinnamoyl]-anthranilic acid (tranilast) inhibits transforming growth factor-beta release and reduces migration and invasiveness of human malignant glioma cells. Int J Cancer 2001;93(1):53–61.

28. Noguchi N, Kawashiri S, Tanaka A, Kato K, Nakaya H. Effects of fibroblast growth inhibitor on proliferation and metastasis of oral squamous cell carcinoma. Oral Oncol 2003;39(3):240–247.
29. Nakanishi H, Takeuchi S, Kato K, Shimizu S, Kobayashi K, Tatematsu M, Shirai T. Establishment and characterization of three androgen-independent, metastatic carcinoma cell lines from 3,2′-dimethyl-4-aminobiphenyl-induced prostatic tumors in F344 rats. Jpn J Cancer Res 1996;87(12):1218–1226.
30. Fukuyama J, Ichikawa K, Miyazawa K, Hamano S, Shibata N, Ujiie A. Tranilast suppresses intimal hyperplasia in the balloon injury model and cuff treatment model in rabbits. Jpn J Pharmacol 1996;70(4):321–327.
31. Kusama H, Kikuchi S, Tazawa S, Katsuno K, Baba Y, Zhai YL, Nikaido T, Fujii S. Tranilast inhibits the proliferation of human coronary smooth muscle cell through the activation of p21waf1. Atherosclerosis 1999;143(2):307–313.
32. Horning JL, Sahoo SK, Vijayaraghavalu S, Dimitrijevic S, Vasir JK, Jain TK, Panda AK, Labhasetwar V. 3-D tumor model for in vitro evaluation of anticancer drugs. Mol Pharm 2008;5(5):849–862.
33. Beningo KA, Dembo M, Wang YL. Responses of fibroblasts to anchorage of dorsal extracellular matrix receptors. Proc Natl Acad Sci USA 2004;101(52):18024–18029.
34. Lee GY, Kenny PA, Lee EH, Bissell MJ. Three-dimensional culture models of normal and malignant breast epithelial cells. Nat Methods 2007;4(4):359–365.
35. Ko SC, Chapple KS, Hawcroft G, Coletta PL, Markham AF, Hull MA. Paracrine cyclooxygenase-2-mediated signalling by macrophages promotes tumorigenic progression of intestinal epithelial cells. Oncogene 2002;21(47):7175–7186.
36. Ramasamy R, Fazekasova H, Lam EW, Soeiro I, Lombardi G, Dazzi F. Mesenchymal stem cells inhibit dendritic cell differentiation and function by preventing entry into the cell cycle. Transplantation 2007;83(1):71–76.
37. Lechner S, Muller-Ladner U, Neumann E, Spottl T, Schlottmann K, Ruschoff J, Scholmerich J, Kullmann F. Thioredoxin reductase 1 expression in colon cancer: Discrepancy between in vitro and in vivo findings. Lab Invest 2003;83(9):1321–1331.
38. Cicenas J. The potential role of Akt phosphorylation in human cancers. Int J Biol Markers 2008;23(1):1–9.
39. Wang Y, Kreisberg JI, Ghosh PM. Cross-talk between the androgen receptor and the phosphatidylinositol 3-kinase/Akt pathway in prostate cancer. Curr Cancer Drug Targets 2007;7(6):591–604.
40. Blanco-Aparicio C, Renner O, Leal JF, Carnero A. PTEN, more than the AKT pathway. Carcinogenesis 2007;28(7):1379–1386.
41. Vene R, Larghero P, Arena G, Sporn MB, Albini A, Tosetti F. Glycogen synthase kinase 3beta regulates cell death induced by synthetic triterpenoids. Cancer Res 2008;68(17):6987–6996.
42. Sharma M, Chuang WW, Sun Z. Phosphatidylinositol 3-kinase/Akt stimulates androgen pathway through GSK3beta inhibition and nuclear beta-catenin accumulation. J Biol Chem 2002;277(34):30935–30941.